

Structure of magnetic separators and separator reconnection

C. E. Parnell,¹ A. L. Haynes,¹ and K. Galsgaard²

Received 12 June 2009; revised 2 August 2009; accepted 11 September 2009; published 26 February 2010.

[1] Magnetic separators are important locations of three-dimensional magnetic reconnection. They are field lines that lie along the edges of four flux domains and represent the intersection of two separatrix surfaces. Since the intersection of two surfaces produces an X-type structure, when viewed along the line of intersection, the global three-dimensional topology of the magnetic field around a separator is hyperbolic. It is therefore usually assumed that the projection of the magnetic field lines themselves onto a two-dimensional plane perpendicular to a separator is also hyperbolic in nature. In this paper, we use the results of a three-dimensional MHD experiment of separator reconnection to show that, in fact, the projection of the magnetic field lines in a cut perpendicular to a separator may be either hyperbolic or elliptic and that the structure of the magnetic field projection may change in space, along the separator, as well as in time, during the life of the separator. Furthermore, in our experiment, we find that there are both spatial and temporal variations in the parallel component of current (and electric field) along the separator, with all high parallel current regions (which are associated with reconnection) occurring between counterrotating flow regions. Importantly, reconnection occurs not only at locations where the structure of the projected perpendicular magnetic field is hyperbolic but also where it is elliptic.

Citation: Parnell, C. E., A. L. Haynes, and K. Galsgaard (2010), Structure of magnetic separators and separator reconnection, *J. Geophys. Res.*, 115, A02102, doi:10.1029/2009JA014557.

1. Introduction

[2] Magnetic reconnection is a fundamental plasma physics process that plays an important role in many solar, magnetospheric, and astrophysical phenomena. Realistic modeling of all these reconnection environments must be done in three dimensions, not simply because they are three dimensional, but, more importantly, because 3-D reconnection is fundamentally different than 2-D reconnection.

[3] In two dimensions, magnetic reconnection can only occur at X-type null points. At the null a pair of field lines with different connectivities, say, $A \rightarrow A'$ and $B \rightarrow B'$, are reconnected to form a new pair of field lines with connectivities $A \rightarrow B'$ and $B \rightarrow A'$. Hence, flux is transferred from one pair of flux domains into another pair of flux domains. Furthermore, in two dimensions, reconnection involves an X-type stagnation flow and results in a discontinuous jump in the field line mapping at the instant reconnection takes place. There has been a considerable body of work on 2-D reconnection, and extensive reviews can be found, for example, in the works by *Priest and Forbes* [2000] and *Biskamp* [2000].

[4] The early research into the nature of 3-D reconnection naturally evolved from the 2-D reconnection work, and various definitions of 3-D reconnection were proposed, including “plasma flows across a surface which separates regions including topologically different magnetic field lines” [*Vasyliunas*, 1975, p. 304], “presence of an electric field along a separator” [*Sonnerup*, 1979, p. 879], “transfer of plasma-elements from one field line to another (i.e., a break down of the frozen-in flux theorem)” [*Axford*, 1984, p. 1], and “evolution in which it is not possible to preserve the global identification of some field lines” (i.e., magnetic field evolution that is not flux preserving) [*Greene*, 1993, p. 2355]. The first two of these definitions require the existence of 3-D magnetic nulls in order to produce the magnetic separatrices and separators which are an essential part of these reconnection scenarios. However, *Schindler et al.* [1988] and *Hesse and Schindler* [1988] proposed a theory of generalized magnetic reconnection in which they established that 3-D reconnection does not require nulls or structures associated with nulls and which encompasses the reconnection definitions previously suggested. In particular, 3-D magnetic reconnection occurs not only at 3-D nulls [e.g., *Craig et al.*, 1995; *Craig and Fabling*, 1996; *Priest and Titov*, 1996; *Pontin and Craig*, 2005; *Pontin and Galsgaard*, 2007; *Pontin et al.*, 2007a, 2007b], but more commonly it occurs in a null-less region of a magnetic field [*Schindler et al.*, 1988; *Hesse and Schindler*, 1988], for instance, in a hyperbolic flux tube [*Priest and Démoulin*, 1995; *Démoulin et al.*, 1996; *Titov et al.*, 2003; *Galsgaard*

¹School of Mathematics and Statistics, University of St. Andrews, Saint Andrews, UK.

²Niels Bohr Institute, Copenhagen, Denmark.

et al., 2003; Linton and Priest, 2003; Aulanier *et al.*, 2005; Pontin *et al.*, 2005a; Aulanier *et al.*, 2006; De Moortel and Galsgaard, 2006a, 2006b; Wilmot-Smith and De Moortel, 2007] or at mode-rational surfaces [Browning *et al.*, 2008; Hood *et al.*, 2009]. Also, recently, Titov *et al.* [2009] have proposed a general method for determining the magnetic reconnection in arbitrary 3-D magnetic configurations. They demonstrate, using their method, that, along with magnetic null points, hyperbolic and cusp minimum points are also favorable sites for magnetic reconnection.

[5] We are concerned in this paper with separator reconnection, and since separators link pairs of opposite-polarity null points, reconnection at a separator has been viewed by many as reconnection involving null points. Separators and separator reconnection have been considered by various authors [e.g., Sonnerup, 1979; Lau and Finn, 1990; Longcope and Cowley, 1996; Galsgaard and Nordlund, 1997; Galsgaard *et al.*, 2000b; Longcope, 2001; Pontin and Craig, 2006; Haynes *et al.*, 2007; Parnell *et al.*, 2008; Dorelli and Bhattacharjee, 2008]. The authors are unaware of any papers that specifically address the importance of the nulls during separator reconnection; this is one of the questions that is addressed in this paper.

[6] Many, but not all, of the above situations depend on the fact that field lines from flux domains with two different connectivities, say, $A \rightarrow A'$ and $B \rightarrow B'$, are reconnected to form field lines in two new flux domains with connectivities $A \rightarrow B'$ and $B \rightarrow A'$, exactly as in the 2-D case. In three dimensions, however, it is generally not possible to identify pairs of field lines that reconnect to form new pairs of field lines [e.g., Hornig and Priest, 2003; Pontin *et al.*, 2005b], apart from nongeneric special cases. Instead, reconnection will occur continually and continuously throughout the finite diffusion region, converting flux from two domains into flux in two other domains. A consequence of this is that, in three dimensions, the field line mapping is, in general, continuous between prereconnected and postreconnected field lines, as opposed to discontinuous. The theory behind this behavior is explained by Hornig and Priest [2003] using a kinematic model and is illustrated very nicely using numerical experiments by Pontin *et al.* [2005a] and Aulanier *et al.* [2006]. From their kinematic model, Hornig and Priest [2003] hypothesize that counterrotating flows are an important ingredient of 3-D reconnection. Also, note that such a flow pattern is implicit within the general reconnection model of Hesse [1995].

[7] Generic magnetic separators are lines which divide four topologically distinct flux domains and hence are locations about which reconnection often occurs. They are the intersection of two separatrix surfaces. (Nongeneric separators involve a spine line from a null, but we ignore these since they are structurally unstable.) Separatrix surfaces are surfaces of field lines that encompass flux from a single source. The field lines in these surfaces originate from nulls, bald edges [Haynes, 2007], or bald patches [Bungey *et al.*, 1996]. The four flux domains surrounding a separator are divided by the two separatrix surfaces. Separators are often termed “X lines” because of the belief that the projection of the magnetic field lines in a 2-D plane perpendicular to the separator has the form of a 2-D X point. Note, however, that the term X line is ambiguous and is also commonly used

for a line of X-type nulls, which is a structurally unstable topological feature [e.g., Hesse and Schindler, 1988]. We therefore do not adopt this term.

[8] The aim of this paper is to determine the main characteristics of separator reconnection. In order to make the work in this paper clear, we first explain our terminology in section 2. For comparative purposes, we then discuss briefly the magnetic field of potential separators (section 3). Our main interest is in investigating the 3-D magnetic field structure of nonpotential separators and, during separator reconnection, the relationship between the magnetic and velocity fields in 2-D planes perpendicular to the separator. To do this, we use a 3-D resistive MHD experiment which is described in section 4. In section 5, we address the following questions: (1) What is the nature of the current density along a separator? (2) Where does reconnection occur along separators? (3) What is the projection of the 3-D magnetic field in a 2-D cut perpendicular to a separator? (4) During reconnection, what is the structure of the 3-D velocity field in the vicinity of a separator? Finally, the conclusions drawn from our results are discussed in section 6.

2. Terminology

[9] In this paper, we investigate the 3-D magnetic and 3-D velocity field structures about separators. Since it is not easy to visualize 3-D magnetic fields in still images, we consider projections of the magnetic field in 2-D planes. In general, such projections can be misleading since the results will differ for each orientation of the projection plane. Thus, to analyze the 3-D magnetic field about a separator at a given point along it, we project the magnetic field onto the unique 2-D plane which is perpendicular to the separator at that point. Thus, we can reliably investigate the 3-D magnetic field both along the length of the separator and also as the separator varies in times. Before we discuss our work, we first define a few terms.

[10] 1. The 3-D topology of a magnetic field is outlined by its magnetic skeleton, which is made up of sources, nulls, separatrix surfaces, and separators. Therefore, the 3-D topological structure is a global phenomenon. Note that here we use the word global to mean “large scale” in a general sense and not as a reference to the whole Sun or magnetosphere.

[11] 2. The 3-D magnetic field structure is defined by the behavior of the magnetic field lines and hence is a local (i.e., “small-scale”) phenomena. The structure may be defined as hyperbolic or elliptic depending on the structure of the 2-D projected field in a perpendicular cross section through the magnetic field: a 2-D saddle (X) or improper fixed point is seen if the 3-D magnetic field structure is hyperbolic, and a 2-D spiral or ellipse (O) is seen if the field structure is elliptic (i.e., has a 3-D helical-type structure).

[12] 3. The 2-D projected field is the projection of the magnetic field in planes perpendicular to the separator. Let \mathbf{B} be any 3-D magnetic field that contains a separator and let \mathbf{x}_0 be a point on the separator with $\hat{\mathbf{n}}_{\parallel}(\mathbf{x}_0)$ as the vector directed along the separator at this point. Then the component of the magnetic field parallel to the separator at \mathbf{x}_0

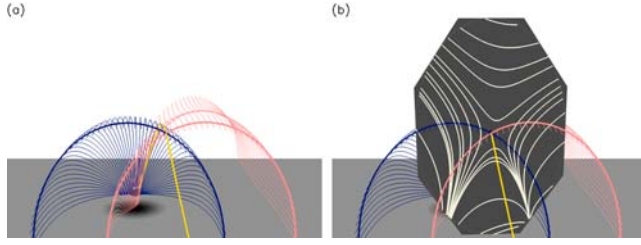


Figure 1. (a) The intersection of the two separatrix surfaces (shown in blue and pink) indicates the X-type nature of the global 3-D topology about a separator (thick yellow line). (b) The 2-D projected field structure in a plane perpendicular to the separator (white lines on grey plane) has a null point which coincides with the point at which the separator pierces the plane. The X-type structure of the 2-D projected field does not coincide with the 3-D global X-type structure formed by the intersection of the two separatrix surfaces.

is given by $\mathbf{B}_{\parallel \mathbf{x}_0} = [\mathbf{B} \cdot \hat{\mathbf{n}}_{\parallel}(\mathbf{x}_0)]\hat{\mathbf{n}}_{\parallel}(\mathbf{x}_0)$, and therefore, the perpendicular magnetic field component is

$$\mathbf{B}_{\perp \mathbf{x}_0} = \mathbf{B} - \mathbf{B}_{\parallel \mathbf{x}_0}. \quad (1)$$

The 2-D projection of the magnetic field in the plane perpendicular to the separator at \mathbf{x}_0 is defined as $\mathbf{B}_{\perp \mathbf{x}_0}$ evaluated in that plane. We call this 2-D projected field $\mathbf{ProjB}_{\perp \mathbf{x}_0}$. Note that the 2-D projected field is not a magnetic field since it does not satisfy the solenoidal constraint, as shown in section 3. The 2-D projected field structure can be defined as hyperbolic or elliptic, using the previously described definitions, depending on the nature of the fixed point in the 2-D projected field where the separator pierces the perpendicular 2-D plane.

[13] In purely 2-D magnetic fields, the magnetic topology and magnetic field line structure coincide, and hence, the 2-D global and local magnetic structures are the same. It is not possible to determine the global magnetic topology of a 3-D magnetic field unless you know the magnetic field in a large number of locations, which is obviously not the case from solar and magnetospheric observations. Instead, estimations of the local 3-D magnetic field and 2-D projections of the magnetic field have been made in magnetospheric physics. In solar physics, images of the solar atmosphere reveal some structure of the magnetic field, as do extrapolations of the local 3-D magnetic field above the photosphere. Here we show that, unlike in two dimensions, the 3-D magnetic topology and local 3-D magnetic field line structure are not the same. Therefore, in order to help with the interpretation of observational (and numerical) results, we investigate what local 3-D magnetic field and 2-D projected field structures are associated with separators.

3. Magnetic Field of a Potential Separator

[14] The 3-D magnetic topology in the vicinity of a separator (potential or nonpotential) is given by the separatrix surfaces that intersect to form the separator. As mentioned in section 2, a cut perpendicular to the separator reveals that the two separatrix surfaces form an “X,” so we describe the

global 3-D magnetic topology in the vicinity of a separator as being hyperbolic (Figure 1a).

[15] In the vicinity of a potential separator, what is the local 3-D magnetic field structure? To answer this question, we need to consider the 2-D projected field structure in planes perpendicular to the separator. By definition, both the divergence and curl of a potential magnetic field are zero, but what are the divergence and curl of the 2-D projected field in cuts perpendicular to the separator?

[16] Let us consider, without loss of generality, a magnetic field, $\mathbf{B}_{\text{pot}} = (B_{px}, B_{py}, B_{pz})$, which has a pair of 3-D nulls at points $(0, 0, a)$ and $(0, 0, b)$ orientated such that their separatrix surfaces intersect along the z axis and a separator lies along this line between $z = a$ and $z = b$. Hence, $\mathbf{B}_{\text{pot}\perp}(x, y, z) = (B_{px}, B_{py}, 0)$ and $\mathbf{B}_{\text{pot}\parallel}(x, y, z) = (0, 0, B_{pz})$. For any point $(0, 0, z_0)$ along the separator, where $a < z_0 < b$, the 2-D projected perpendicular field is $\mathbf{ProjB}_{\text{pot}\perp z_0}(x, y) = \mathbf{B}_{\text{pot}\perp}(x, y, z_0)$; hence, its components are functions of x and y but not z . Thus, the divergence of the 2-D projected field becomes

$$\begin{aligned} \nabla \cdot \mathbf{ProjB}_{\text{pot}\perp z_0}(x, y) &= \frac{\partial B_{px}(x, y, z_0)}{\partial x} + \frac{\partial B_{py}(x, y, z_0)}{\partial y} \\ &\neq 0 \end{aligned}$$

since

$$\left. \frac{\partial B_{pz}(x, y, z)}{\partial z} \right|_{z=z_0} \neq 0.$$

Therefore $\mathbf{ProjB}_{\text{pot}\perp z_0}$ is not a magnetic field, but simply a 2-D vector field. Now, the curl of $\mathbf{ProjB}_{\text{pot}\perp z_0}(x, y)$ is

$$\begin{aligned} \nabla \times \mathbf{ProjB}_{\text{pot}\perp z_0}(x, y) &= \left(0, 0, \frac{\partial B_{py}(x, y, z_0)}{\partial x} - \frac{\partial B_{px}(x, y, z_0)}{\partial y} \right) \\ &= (0, 0, 0) \end{aligned}$$

since the 3-D magnetic field is potential. We note here that the curl of the projected magnetic field and the projection of the curl of the magnetic field are not commutative, and hence the result above is true for potential fields.

[17] Thus, in general, if one linearized $\mathbf{ProjB}_{\text{pot}\perp z_0}(x, y)$ about the point $(0, 0)$ through which the separator pierces the plane, the magnetic field would have the form

$$\mathbf{ProjB}_{\text{pot}\perp z_0}(x, y) \approx \begin{bmatrix} a & c/2 \\ c/2 & b \end{bmatrix} \begin{pmatrix} x \\ y \end{pmatrix}. \quad (2)$$

The eigenvalues of this field are

$$\lambda_{\pm} = \frac{a+b}{2} \pm \frac{1}{2} \sqrt{(a-b)^2 + c^2},$$

so they are always real. This means the structure of the local 2-D projected field in a plane perpendicular to a potential separator can be either an X point, a stable or unstable proper node (star), or a stable or unstable improper node depending on the relative values of a , b , and c .

[18] Now, if the 2-D plane perpendicular to the separator is at either of the 3-D nulls at the ends of the separator, the X-type 2-D projected field structure will coincide with the X-type structure formed by the 3-D separatrix surfaces. It has long been believed that this holds true along the com-

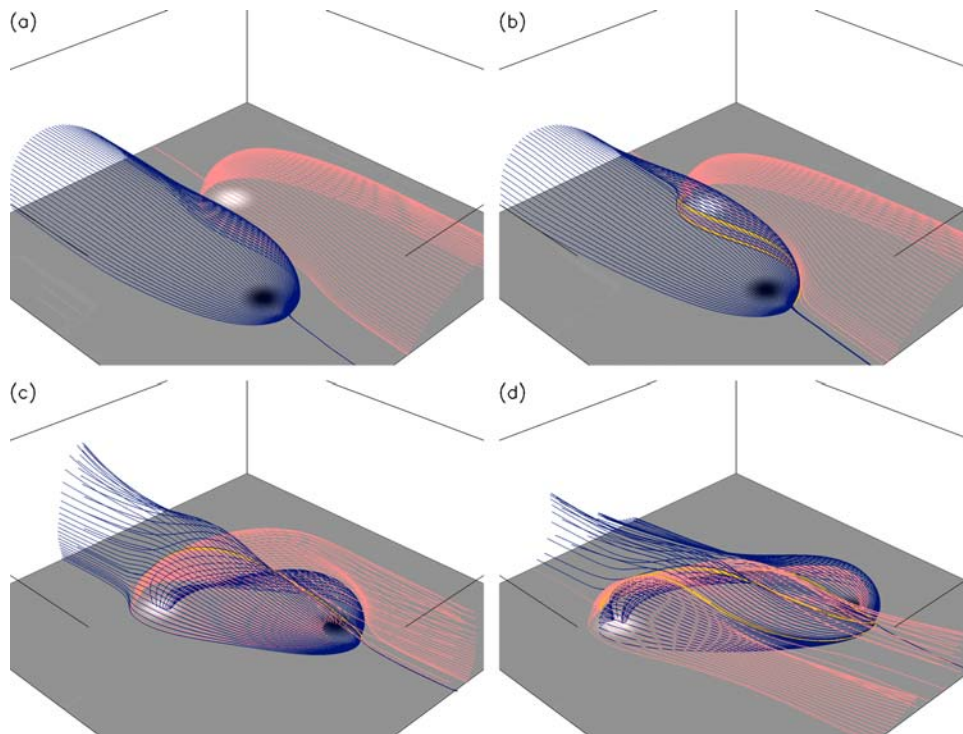


Figure 2. Snapshots showing the nonpotential magnetic skeleton of our model at times (a) $t = 2.53$, (b) $t = 4.50$, (c) $t = 13.47$, and (d) $t = 17.85$, including the positive and negative sources on the base (white and black discs), the positive and negative separatrix surfaces (pink and blue surfaces), and separators (thick yellow lines).

plete length of the separator; however, as we have just shown, this is not necessarily the case since, for some portion of the separator, the projection of the 2-D perpendicular field may look like a star or an improper fixed point. Furthermore, the two separatrix surfaces forming the separator do not necessarily intersect at right angles along the complete length of the separator, so the global 3-D topology does not necessarily form a right-angled “X.” However, if the 2-D projected field structure is a saddle, then this X structure must be right angled since $\nabla \times \mathbf{ProjB}_{\text{pot}\perp} = 0$. Thus, these two X-type structures cannot always coincide, as shown in Figure 1b. Therefore, the 2-D projected field structure in a plane perpendicular to the separator does not necessarily reflect the global 3-D magnetic topology of the field. Hence, the local 3-D magnetic field structure and global 3-D magnetic topology do not necessarily coincide either.

[19] In light of this rather surprising discovery about the nature of the local 3-D magnetic field structure in the vicinity of a potential separator, we now go on to consider nonpotential separators and separator reconnection. To do this, we use results from a numerical experiment which we briefly review as a whole in section 4 before focusing on the details of the separators in this experiment in section 5.

4. Three-Dimensional Numerical Model

[20] The 3-D numerical setup used here is very similar to that used by *Galsgaard et al.* [2000a], *Haynes et al.* [2007],

Parnell et al. [2008], and A. L. Haynes et al. (The effects of magnetic resistivity on a magnetic flyby model, manuscript in preparation, 2010), so we only give a very brief description here. We consider a Cartesian grid of $256 \times 256 \times 129$ scaled to $1 \times 1 \times 1/4$. The initial magnetic field is potential and involves two sources of finite extent on the base of the box which contain equal amounts of flux but are of opposite polarity. An overlying field is then added in the \hat{y} direction to ensure that the sources are initially disconnected. The side boundaries of the box are periodic, while the top boundary is closed. On the base, the boundary is closed apart from the two sources. The sources are driven along lanes, at a speed of 0.02 of the initial peak Alfvén speed in the box, such that they run antiparallel to each other in a direction perpendicular to the overlying field (the \hat{x} direction), resulting in the interaction of their fluxes by way of reconnection at a series of separators. The drivers are switched off before the sources leave the box at 26.7 Alfvén crossing times (where the crossing time of the box is determined from the peak Alfvén speed). We start with a uniform atmosphere which has an initial density and pressure of $1/4$ and $1/6$, respectively, in dimensionless units.

[21] The numerical code is a resistive MHD code which has a staggered grid and uses sixth-order spatial derivatives with fifth-order interpolation. Time is advanced by a third-order predictor-corrector method. In this paper, we consider an experiment in which the magnetic resistivity is held constant at 6.25×10^{-5} . The Lundquist number for the experiment is 18,693 (determined from the same values as the Alfvén crossing time). However, the local magnetic

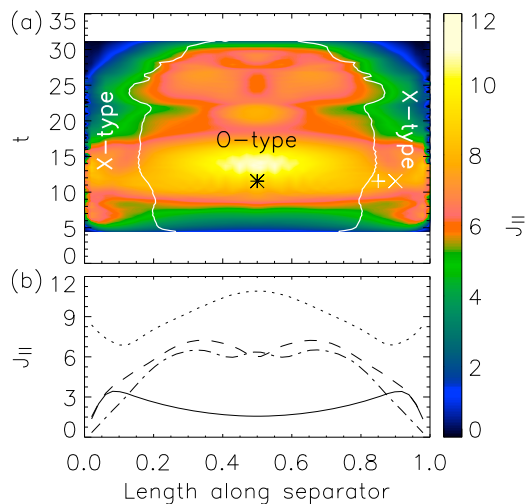


Figure 3. (a) Contour plot of current parallel to separator. The x axis is the normalized length along the separator, and the y axis is time. The white lines indicate when the 2-D perpendicular magnetic field structure changes from X-type to O-type. The symbols mark the points where the 2-D perpendicular projections in Figure 5 were taken. (b) Current parallel to the separator versus length along the separator at $t = 4.78$ (solid line), 14.03 (dotted line), 25.74 (dashed line), and 28.16 (dash-dotted line) Alfvén times.

Reynolds number within our domain can vary greatly from order unity up to several thousand.

5. Separators and Separator Reconnection

[22] The magnetic configuration in our experiment involves two magnetic nulls on the base of the box which remain for the entire experiment. The initial setup is shown in Figure 2a and contains no separators. However, the boundary driving motions lead to the creation of a number of separators linking the two nulls, as described by *Haynes et al.* [2007]. In particular, the first separators created are a pair formed by a global double-separator bifurcation, as shown in Figure 2b. The lower of these two separators rapidly disappears at the base of the box, leaving the upper separator, which lasts for most of the experiment. This separator is visible in Figures 2c and 2d (central separator). It is this separator that we investigate in detail. Further separators are formed (Figure 2d), but since their characteristics are similar to the one we are focusing on we do not discuss them in detail.

5.1. Nature of the Current Along a Reconnecting Separator

[23] In separator reconnection the rate of reconnection is related to the amount of electric field parallel to the separator [*Sonnerup, 1979; Hesse and Birn, 1993; Hesse, 1995; Parnell et al., 2008*]. When the resistivity η is constant, the parallel electric field is simply related to the parallel electric current by a factor η . Thus, studying the nature of the parallel current along the separator reveals where, along the length of the separator, reconnection is actually occurring.

[24] Figure 3a shows a contour plot of the parallel current along the length of the separator varying in time. Clearly, the current (and hence the reconnection) is neither constant

in time nor constant along the length of the separator. Initially ($t = 4.78$), the current grows from two locations near the ends of the separator but not at the nulls (Figure 3b). The current then spreads out along the separator and increases in intensity. At about 14.03 Alfvén times the current peaks near the center of the separator. Later on (during a phase including further separators) the currents are seen to have a double ($t = 25.74$) and triple ($t = 28.16$) peaked nature (Figure 3b).

5.2. Where Does Reconnection Occur Along Separators?

[25] The reconnection along the separator occurs where there are high parallel currents and, hence, high parallel electric fields. From our analysis it is clear that separator reconnection does not (only) occur at the nulls at the ends of the separator but that the vast majority occurs in one or more localized regions along its length. In our experiment there are periods with what appear to be two or three enhanced regions of reconnection along a single separator, as well as periods where there is just one site extending over much of the length of the separator (Figure 3).

[26] The reconnection rate r_{sep} at the separator is given by the formula [*Hesse and Birn, 1993; Hesse, 1995; Hornig and Priest, 2003; Parnell et al., 2008*]

$$r_{\text{sep}} = \frac{d\phi}{dt} = \int_l E_{\parallel} dl = \eta \int_l j_{\parallel} dl, \quad (3)$$

where E_{\parallel} and j_{\parallel} are the components of the electric field and electric current parallel to the separator, respectively, and l is the distance along the separator. This rate is equivalent to the rate of change of flux ϕ within any one of the four surrounding flux domains of the separator due to the reconnection at this separator. In Figure 4, we have plotted r_{sep} (solid line) against time, showing that the total reconnection along this separator varies considerably in time and shows two distinct peak rates. The first peak in reconnection rate occurs when there is a single large current sheet along the center portion of the separator. The second peak occurs when there are two or three distinct high-current regions along the separator. So, of course, what matters is not simply what the highest parallel current is along the sepa-

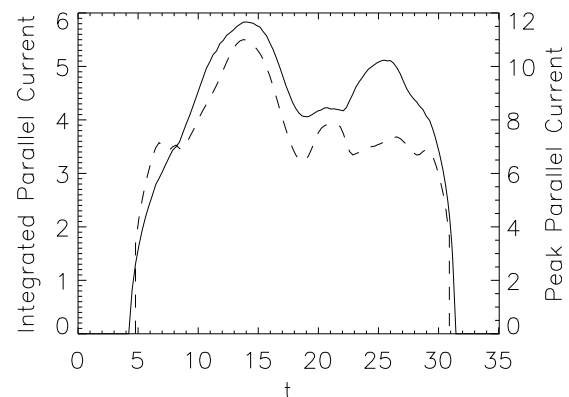


Figure 4. Reconnection rate given by the integrated parallel electric field along the separator (solid line) and peak parallel electric field (dashed line) versus time.

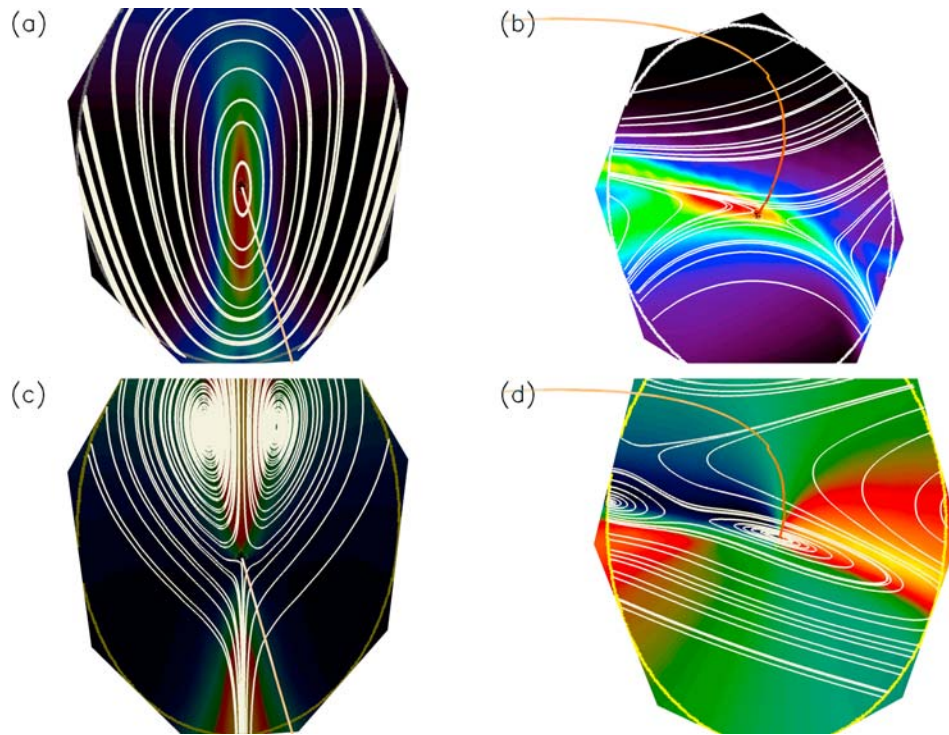


Figure 5. Plots showing (top) the 2-D projected field structure (white lines) and (bottom) the 2-D velocity field structure (white lines) in perpendicular planes at (a) 0.5, (b) 0.9, (c) 0.5, and (d) 0.85 along the separator at time $t = 13.47$. The separator (thick line coming out of the plane) is shaded according to its parallel current (current, red; temperature (low and high), black and white). The contours on the surface perpendicular to the separator show the absolute current in the plane (Figures 5a and 5b) (low (black) to high (red)) and the radial velocity in the plane with respect to the point at which the separator pierces the plane (Figures 5c and 5d) (inflow, blue and green; outflow, red and yellow).

rator (dashed line in Figure 4) but the extent of the region(s) over which the parallel current is high (i.e., the size of the overall reconnection site).

5.3. Projected 3-D Magnetic Field in a 2-D Cut Perpendicular to the Separator

[27] We have already seen in section 2 that for potential fields, the global 3-D magnetic topology and local 3-D magnetic field structures do not necessarily coincide. Here we consider what the local 3-D magnetic field structure is about a nonpotential separator by looking at \mathbf{ProjB}_{\perp} , the 2-D projected field perpendicular to it.

[28] The magnetic field in the vicinity of a separator typically has a strong component parallel to the direction of the separator, although this is not true near the ends of the separator. Again, we use equation (1) to determine the 2-D projected field in a plane perpendicular to the separator, and we recall that this 2-D field has a null at the point where the separator pierces the plane.

[29] We have already found that the 2-D projected field structure in a plane perpendicular to a potential separator can be an X-type or a proper or improper node since the linear field always has real eigenvalues. In the nonpotential case, though, there are likely to be currents parallel to the separator as there are during separator reconnection. We find, using the same notation as equation (2), that, to first order, the 2-D projected field \mathbf{ProjB}_{\perp} about the 2-D null point at

which the separator pierces the plane, located at the origin for simplicity, has the form

$$\mathbf{ProjB}_{\perp} = \begin{bmatrix} a & (c - j_{\parallel})/2 \\ (c + j_{\parallel})/2 & b \end{bmatrix} \begin{pmatrix} x_1 \\ x_2 \end{pmatrix}, \quad (4)$$

where x_1 and x_2 are orthogonal coordinates lying in the 2-D perpendicular plane. The 2-D null will have real eigenvalues if $(a - b)^2 + c^2 > j_{\parallel}^2$ (creating an X point or a proper or improper node), and the field will have complex eigenvalues if $(a - b)^2 + c^2 < j_{\parallel}^2$ (creating a spiral or O-type node), where j_{\parallel} is the component of current out of the plane. Hence, linear 2-D projected fields are typically spiral or O-type if the current is large (relative to the other components in the matrix). Therefore, \mathbf{ProjB}_{\perp} about a nonpotential separator could take on one of many forms, and its structure is likely to vary along the separator.

[30] Plots of \mathbf{ProjB}_{\perp} determined at 1/2 (Figure 5a) and 9/10 (Figure 5b) of the way along the separator at $t = 13.47$ reveal that, indeed, the 2-D projected field structure perpendicular to our separator does change in nature along the length of the separator. \mathbf{ProjB}_{\perp} is of O type near the center of the separator while it appears to be of X type near its end. The asterisk and plus in Figure 3 indicate the points where the above two 2-D perpendicular plots were taken. We determined the nature of \mathbf{ProjB}_{\perp} at every point along our separator for every time step and overplotted white

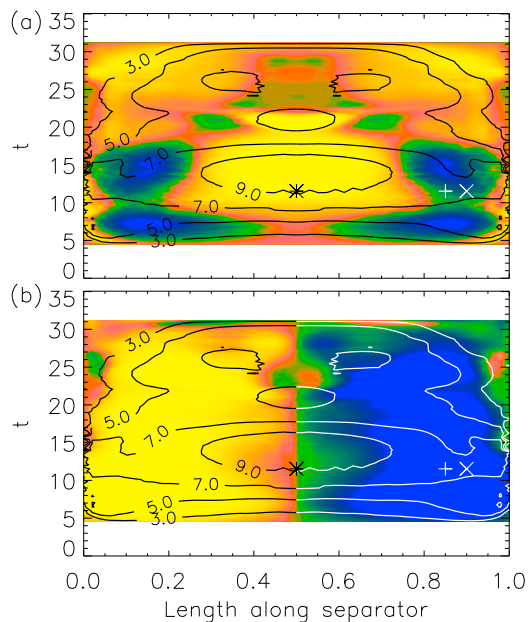


Figure 6. (a) The discriminant of \mathbf{Projv}_\perp , where blue and green imply spiral or O-type flow and yellow and red imply an improper or X-type flow. (b) The curl of \mathbf{Projv}_\perp (yellow and red, positive; blue and green, negative). Both plots have contours of E_\parallel (or j_\parallel) overplotted. The symbols mark the points where the 2-D perpendicular projections in Figure 5 were taken.

lines in Figure 3 where the nature of \mathbf{ProjB}_\perp changes. These lines reveal that for the entire life of our separator its perpendicular 2-D projected field structure has real eigenvalues (e.g., is of X type) near the ends of the separator and has complex eigenvalues (e.g., is either spiral or O-type) in the middle, although the length of this complex eigenvalue region changes in time (note that the other two long-lived separators in our experiment show a similar pattern for \mathbf{ProjB}_\perp). Indeed, for all generic separators (separators created by the intersection of two separatrix surfaces) which have a null at either end, \mathbf{ProjB}_\perp must have an X-type nature at the ends of the separator, so it is not a surprise that our separators show this feature. The spiral or O-type nature in the middle can be explained by the fact that our two separatrix surfaces are driven such that they entwine around each other even though our driving flow is just a simple shear flow. Thus, even though the global 3-D topology of the magnetic field near the separator is always X-type, the local 3-D magnetic field structure about the separator can be either hyperbolic or elliptic along different regions of the same separator. Also, the local 3-D field structure can change its nature in time.

5.4. Structure of the 3-D Velocity About a Reconnecting Separator

[31] The specific locations along the separator that have high currents should be the locations where the flux is reconnecting fastest. From Figure 3, it can be seen that these locations do not coincide exclusively with spiral or O-type perpendicular fields; however, many of them do. Thus, hyperbolic local 3-D magnetic field structures are not essential for reconnection: elliptic ones are also pos-

sible reconnection sites. Therefore, knowing the local 3-D structure of a magnetic field does not allow us to identify a separator or separator reconnection, but is there anything special about the local 3-D velocity structure that can allow us to identify possible separator reconnection?

[32] From the induction equation, which describes the rate of change of the magnetic field, one can see that reconnection requires not only high currents to produce a diffusion region but also a velocity flow that carries the magnetic field through the ideal region into the diffusion region. Thus, we also consider what the nature of the 2-D projected velocity structure perpendicular to the separator is, where \mathbf{Projv}_\perp is equal to \mathbf{v}_\perp evaluated in the perpendicular plane and $\mathbf{v}_\perp = \mathbf{v} - (\mathbf{v} \cdot \hat{\mathbf{n}}_\parallel)\hat{\mathbf{n}}_\parallel$. In Figures 5c and 5d, we show two plots of \mathbf{Projv}_\perp (lines) relative to the separator taken at the same time as the two graphs in Figures 5a and 5b. In Figure 5c, where the parallel current (hence parallel electric field) is high (indicated by the asterisk in Figure 3), and thus reconnection is strong, the projection of the streamlines onto this plane reveals an X-type stagnation flow within the immediate vicinity of the separator. However, where reconnection is slower (i.e., the parallel current and electric field are low, as indicated by the cross in Figure 3), we have an O-type stagnation flow (Figure 5d). The contours in Figures 5c and 5d reveal the radial flow from the separator in the plane and show that both flows can give rise to distinct narrow outflow jets associated with the reconnection.

[33] The blue and green filled contours in Figure 6a indicate on a time-distance graph where the 2-D perpendicular velocity structure has complex eigenvalues (spiral or O type), and the red and yellow filled contours indicate where they are real (improper or X type). In comparison with \mathbf{E}_\parallel (contour lines in Figure 6a) the 2-D perpendicular velocity structure is of improper or X type in the regions where the electric field is largest. However, the 2-D perpendicular velocity structure is not of improper or X type along the complete length of the separator. This seems to imply that for 3-D reconnection it is not essential to have a 2-D perpendicular X-type stagnation flow; instead, a 2-D perpendicular spiral or O-type stagnation flow is possible.

[34] Thus, we consider what other characteristic of the velocity may be important for reconnection. In particular, following *Hornig and Priest* [2003], we look for counterrotating flows on either side of the main reconnection region. Figure 6b shows a contour plot of $(\nabla \times \mathbf{Projv}_\perp) \cdot \mathbf{n}_\parallel$. Red and yellow indicate $(\nabla \times \mathbf{Projv}_\perp) \cdot \mathbf{n}_\parallel > 0$, and green and blue indicate $(\nabla \times \mathbf{Projv}_\perp) \cdot \mathbf{n}_\parallel < 0$. The change of the sign of $(\nabla \times \mathbf{Projv}_\perp) \cdot \mathbf{n}_\parallel$ on either side of the center of the separator, where the highest E_\parallel (or j_\parallel) occurs, indicates counterrotating flows.

[35] Interestingly, in the center of the separator the dividing line between the two counterrotating regions appears to broaden (e.g., between 8–16 Alfvén times and 22–27 Alfvén times (Figure 6b)), and these times coincide with peaks in the reconnection rate, as shown in Figure 4. The first broad region corresponds to the single large peak in j_\parallel at that time. However, between 22 and 27 Alfvén times j_\parallel is doubly peaked, and the broadening in the division between the counterrotating regions appears more like a series of multiple counterrotating regions with the two most distinct divisions between the two counterrotating flows coinciding with the two peaks in j_\parallel . This supports the

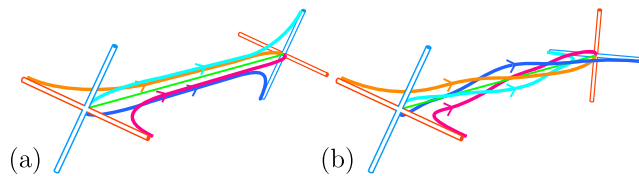


Figure 7. Cartoons showing the 3-D global magnetic topology about (a) a separator with a hyperbolic local 3-D field structure and (b) a separator with an elliptic local 3-D magnetic field structure (equivalent to the separator in Figure 7a twisted by $3\pi/2$). Each cartoon includes a separator (green), three field lines lying in the separatrix surface of the near null (blue, cyan, and the straight blue edge from the near null), three field lines lying in the separatrix surface of the far null (pink, orange, and the straight orange edge from the far null), a spine from the near null (straight orange edge), and a spine from the far null (straight blue edge).

idea that reconnection at a separator does not occur at a single location but occurs over an extended region and that it might even occur at multiple “hot spots” along the separator.

6. Conclusions

[36] In purely 2-D magnetic fields, the magnetic topology and magnetic field line structure coincide, and hence, the 2-D global and local magnetic structures are the same. We show that for 3-D magnetic fields, the global 3-D topological structures and the local 3-D field structures do not coincide. This is important since it is not possible to determine the 3-D global magnetic topology of a magnetic field unless you know the magnetic field practically everywhere, which is obviously not the case from solar and magnetospheric observations. Thus, identifying separators in observations is difficult.

[37] Here we determine the nature of separators and separator reconnection in the hope of finding characteristics that can be used to identify them without determining the full topology of the field. From our studies, we conclude the following important features of separator reconnection.

[38] 1. The parallel electric current (parallel electric field) along a separator varies both spatially and temporally. The parallel electric field along the length of a separator is not necessarily constant. It may be multiply peaked, with the highest peaks seen along the length of the separator away from its ends (null points).

[39] 2. Reconnection occurs in local hot spots of current along separators. There may be either single or multiply enhanced locations of reconnection along a separator.

[40] 3. Separators may have a 3-D local magnetic field structure that is X type or spiral or O type in planes perpendicular to the separator. The global 3-D magnetic topology about a generic separator (potential or nonpotential) is, by definition, X type (given by the intersection of the two separatrix surfaces that form the separator). The 2-D projected field structure perpendicular to the separator may be either X type, improper node, spiral, or O type for nonpotential separators and can be either X-type or improper for potential separators. Furthermore, if the local 2-D perpendicular magnetic field structure is X-type, then this local X-type structure will not necessarily coincide with the

global X-type structure given by the field’s magnetic topology. In Figure 7, we have sketched a pair of cartoons to illustrate what a separator with a local X-type projected perpendicular 2-D field (Figure 7a) and a local O-type projected perpendicular field (Figure 7b) look like. All that is different between these two separators is that Figure 7b is produced by rotating Figure 7a at the far end by $3\pi/2$. However, in the numerical experiment discussed here, the ends of the separator were fixed at the two nulls situated on the base, and neither of these actually rotate during the experiment, so the creation of an elliptic local 3-D magnetic field structure is not necessarily created by a physical rotation of the separator; this is simply how it may be visualized.

[41] 4. Separator reconnection occurs between regions with counterrotating flow. *Hornig and Priest* [2003] hypothesized that counterrotating flows are important for 3-D reconnection, and our numerical experiment confirms the importance of these flows. Indeed, the locations along a separator which show the strongest parallel electric field lie between regions of counterrotating flows, and the wider the division between the two strong counterrotational regions, the greater the reconnection at that time and in that location along the separator. In general, these regions also show a 2-D X-type stagnation flow perpendicular to the separator.

[42] 5. Separator reconnection does not (only) involve null point reconnection. We find that separator reconnection is distinct from null point reconnection and does not seem to involve reconnection at the null points at the ends of the separator.

[43] The implications from these results change a number of long-held ideas. In particular, the idea suggested by *Priest and Forbes* [1989] that magnetic fields with a hyperbolic 3-D magnetic field structure are important potential locations for reconnection is not the whole story. Magnetic fields whose 3-D magnetic field structure is locally elliptic in nature are equally (maybe even more) important for reconnection and thus should not be ignored. What is important for magnetic reconnection involving a change of connectivity of magnetic flux is that the global 3-D topology (rather than the local 3-D magnetic structure) of the magnetic field is X-type and thus allows changes to the global structure of the magnetic field. However, determining the topology of the magnetic field is not easy, and as yet separatrix surfaces cannot simply be “observed.” Thus, many had taken to looking for X-type projections of the 3-D magnetic field in a plane. However, this work shows that the most important reconnection locations are likely to be located in regions which show an O-type projection of the magnetic field. This should not be surprising since separator reconnection involves a current along the separator and, if strong enough, then such a current will generate a dominant circular magnetic field component.

[44] Furthermore, *Priest and Forbes* [1989] also suggested that an important ingredient for magnetic reconnection was a local 2-D X-type stagnation flow. However, probably more important is the existence of counterrotating flows, as suggested by *Hornig and Priest* [2003], although strong outflow jets are still found from the reconnection sites along the separator.

[45] In this study, we have considered reconnection about a separator that is anchored on the base of our box. If, instead, we cut off our box a few grid points higher so our domain still contained the remains of the separator but there

were no longer any nulls within our domain, we would effectively have created a quasi-separator. Since the reconnection found in our experiment occurs along the separator and not at the nulls, we would expect reconnection to occur in much the same way along our quasi-separator. Thus, we suspect that reconnection about quasi-separators is likely to be very similar [Titov *et al.*, 2003; Wilmot-Smith and De Moortel, 2007]. For instance, Wilmot-Smith and De Moortel [2007] found that in the middle of their quasi-separator, where much of their reconnection was occurring, the 2-D perpendicular magnetic field was elliptic in nature and there was some evidence of counterrotational flows, although in some sense these flows arise simply from the pattern of their driver. However, it is not clear that this is an essential ingredient for 3-D reconnection. Further studies need to be undertaken to investigate the nature of other types of reconnecting magnetic structures.

[46] Finally, we consider whether the magnetic structure of separators can be observed. The magnetic field in the magnetosphere is observed using in situ measurements. For example, Cluster has four spacecraft and hence can determine all three components of the magnetic field at four locations in the magnetosphere simultaneously. Depending on the size of the separator and the extent of the local magnetic field structure about it, it may be possible to identify regions that show a 3-D helical-like structure, i.e., with two components of the magnetic field indicating a circular field and the third indicating a single field direction. Evidence of a traditional hyperbolic separator has been found using Cluster data [e.g., Phan *et al.*, 2006]; however, as far as the authors know, elliptical separator field patterns have not yet been sought. Looking for these might be interesting as they are the natural occurrence of a high parallel electric field in which reconnection is very likely to occur, but, of course, they may not be visible if the helical structure of the field is very localized.

[47] In the solar corona, the magnetic field structure is inferred from X-ray or UV images. Since the corona is optically thin, all the plasma of a given temperature along the line of site is observed. Hence, the resulting images show particular magnetic structures, or parts of structures, flattened onto the plane of sky. This means magnetic structures at a different temperature cannot be seen or observable structures may be obscured from view by other observable plasma. Furthermore, structures will appear different depending on the particular plane of sky orientation observed (e.g., see the projections of CME magnetic fields from the numerical model by Tokman and Bellan [2002]). Therefore, identifying, for example, helical structures will not be easy. Moreover, the sections of the separators that have a locally helical field line structure are the regions that have the highest parallel electric fields and are where most of the magnetic reconnection is occurring. In such regions, prereconnected field lines may not be visible if they are too cool, and postreconnected field lines will be transported out of the reconnection site because of the strong outflow from the reconnection, so they too may not reveal a helical structure. Finally, the local structure about the separator may be too small to observe with the current image resolution. In order to properly determine the structures we might expect to see in the corona in the vicinity of a separator, we need to forward model the results from a series of

numerical experiments involving separators and calculate coronal images from various angles. This is outside the scope of the current paper.

[48] **Acknowledgments.** C.E.P. and A.L.H. would like to thank the Leverhulme Trust: C.E.P. was awarded a Philip Leverhulme Prize in 2007 which she is using to support A.L.H. as a research associate. Support by the European Commission through the Solaire Network (MTRN-CT-2006-035484) is gratefully acknowledged. The authors would like to thank Thomas Neukirch and Eric Priest for helpful suggestions in improving this manuscript.

[49] Amitava Bhattacharjee thanks Terry Forbes and another reviewer for their assistance in evaluating this paper.

References

- Aulanier, G., E. Pariat, and P. Démoulin (2005), Current sheet formation in quasi-separatrix layers and hyperbolic flux tubes, *Astron. Astrophys.*, *444*, 961–976, doi:10.1051/0004-6361:20053600.
- Aulanier, G., E. Pariat, P. Démoulin, and C. R. DeVore (2006), Slip-running reconnection in quasi-separatrix layers, *Sol. Phys.*, *238*(2), 347–376, doi:10.1007/s11207-006-0230-2.
- Axford, W. I. (1984), Magnetic field reconnection, in *Magnetic Reconnection in Space and Laboratory Plasmas*, *Geophys. Monogr. Ser.*, vol. 30, edited by E. W. Hones Jr., pp. 1–8, AGU, Washington, D. C.
- Biskamp, D. (2000), *Magnetic Reconnection in Plasmas*, Cambridge Univ. Press, Cambridge, U. K.
- Browning, P. K., C. Gerrard, A. W. Hood, R. Kevis, and R. A. M. Van der Linden (2008), Heating the corona by nanoflares: Simulations of energy release triggered by a kink instability, *Astron. Astrophys.*, *485*, 837–848, doi:10.1051/0004-6361:20079192.
- Bunge, T. N., V. S. Titov, and E. R. Priest (1996), Basic topological elements of coronal magnetic fields, *Astron. Astrophys.*, *308*, 233–247.
- Craig, I. J. D., and R. B. Fabling (1996), Exact solutions for steady state, spine, and fan magnetic reconnection, *Astrophys. J.*, *462*, 969–976, doi:10.1086/177210.
- Craig, I. J. D., R. B. Fabling, S. M. Henton, and G. J. Rickard (1995), An exact solution for steady state magnetic reconnection in three dimensions, *Astrophys. J.*, *455*, L197, doi:10.1086/309822.
- De Moortel, I., and K. Galsgaard (2006a), Numerical modeling of 3D reconnection due to rotational foot point motions, *Astron. Astrophys.*, *451*, 1101–1115, doi:10.1051/0004-6361:20054587.
- De Moortel, I., and K. Galsgaard (2006b), Numerical modeling of 3D reconnection: II. Comparison between rotational and spinning foot point motions, *Astron. Astrophys.*, *459*, 627–639, doi:10.1051/0004-6361:20065716.
- Démoulin, P., E. R. Priest, and D. P. Lonie (1996), Three-dimensional magnetic reconnection without null points: 2. Application to twisted flux tubes, *J. Geophys. Res.*, *101*, 7631–7646, doi:10.1029/95JA03558.
- Dorelli, J. C., and A. Bhattacharjee (2008), Defining and identifying three-dimensional magnetic reconnection in resistive magnetohydrodynamic simulations of Earth's magnetosphere, *Phys. Plasmas*, *15*, 056504, doi:10.1063/1.2913548.
- Galsgaard, K., and Å Nordlund (1997), Heating and activity of the solar corona: 3. Dynamics of a low beta plasma with three-dimensional null points, *J. Geophys. Res.*, *102*, 231–248, doi:10.1029/96JA02680.
- Galsgaard, K., C. E. Parnell, and J. Blaizot (2000a), Elementary heating events—Magnetic interactions between two flux sources, *Astron. Astrophys.*, *362*, 395–405.
- Galsgaard, K., E. R. Priest, and Å Nordlund (2000b), Three-dimensional separator reconnection—How does it occur?, *Sol. Phys.*, *193*, 1–16, doi:10.1023/A:1005248811680.
- Galsgaard, K., V. S. Titov, and T. Neukirch (2003), Magnetic pinching of hyperbolic flux tubes. II. Dynamic numerical model, *Astrophys. J.*, *595*, 506–516, doi:10.1086/377258.
- Greene, J. M. (1993), Reconnection of vorticity lines and magnetic lines, *Phys. Fluids B*, *5*, 2355–2362, doi:10.1063/1.860718.
- Haynes, A. L. (2007), Magnetic skeletons and 3D magnetic reconnection, Ph.D. thesis, Univ. of St. Andrews, Saint Andrews, U. K.
- Haynes, A. L., C. E. Parnell, K. Galsgaard, and E. R. Priest (2007), Magnetohydrodynamic evolution of magnetic skeletons, *Proc. R. Soc. A*, *463*, 1097–1115.
- Hesse, M. (1995), Three-dimensional magnetic reconnection in space- and astrophysical plasmas and its consequences for particle acceleration, in *Cosmic Magnetic Fields*, *Rev. Mod. Astron.*, vol. 8, edited by G. Klare, pp. 323–348, Springer, Berlin.

- Hesse, M., and J. Birn (1993), Parallel electric fields as acceleration mechanisms in three-dimensional magnetic reconnection, *Adv. Space Res.*, *13*, 249–252, doi:10.1016/0273-1177(93)90341-8.
- Hesse, M., and K. Schindler (1988), A theoretical foundation of general magnetic reconnection, *J. Geophys. Res.*, *93*, 5559–5567, doi:10.1029/JA093iA06p05559.
- Hood, A. W., P. K. Browning, and R. A. M. van der Linden (2009), Coronal heating by magnetic reconnection in loops with zero net current, *Astron. Astrophys.*, *506*, 913–925, doi:10.1051/0004-6361/200912285.
- Hornig, G., and E. R. Priest (2003), Evolution of magnetic flux in an isolated reconnection process, *Phys. Plasmas*, *10*, 2712–2721.
- Lau, Y.-T., and J. Finn (1990), Three-dimensional kinematic reconnection in the presence of field nulls and closed field lines, *Astrophys. J.*, *350*, 672–691.
- Linton, M. G., and E. R. Priest (2003), Three-dimensional reconnection of untwisted magnetic flux tubes, *Astrophys. J.*, *595*, 1259–1276, doi:10.1086/377439.
- Longcope, D. W. (2001), Separator current sheets: Generic features in minimum-energy magnetic fields subject to flux constraints, *Phys. Plasmas*, *8*, 5277–5290, doi:10.1063/1.1418431.
- Longcope, D. W., and S. C. Cowley (1996), Current sheet formation along three-dimensional magnetic separators, *Phys. Plasmas*, *3*, 2885–2897, doi:10.1063/1.871627.
- Parnell, C. E., A. L. Haynes, and K. Galsgaard (2008), Recursive reconnection and magnetic skeletons, *Astrophys. J.*, *675*, 1656–1665, doi:10.1086/527532.
- Phan, T. D., et al. (2006), A magnetic reconnection X-line extending more than 390 Earth radii in the solar wind, *Nature*, *439*, 175–178.
- Pontin, D. I., and I. J. D. Craig (2005), Current singularities at finitely compressible three-dimensional magnetic null points, *Phys. Plasmas*, *12*, 072112, doi:10.1063/1.1987379.
- Pontin, D. I., and I. J. D. Craig (2006), Dynamic three-dimensional reconnection in a separator geometry with two null points, *Astrophys. J.*, *642*, 568–578.
- Pontin, D. I., and K. Galsgaard (2007), Current amplification and magnetic reconnection at a three-dimensional null point: Physical characteristics, *J. Geophys. Res.*, *112*, A03103, doi:10.1029/2006JA011848.
- Pontin, D. I., K. Galsgaard, G. Hornig, and E. R. Priest (2005a), A fully magnetohydrodynamic simulation of three-dimensional non-null reconnection, *Phys. Plasmas*, *12*, 052307, doi:10.1063/1.1891005.
- Pontin, D. I., G. Hornig, and E. R. Priest (2005b), Kinematic reconnection at a magnetic null point: Fan-aligned current, *Geophys. Astrophys. Fluid Dyn.*, *99*, 77–93.
- Pontin, D. I., A. Bhattacharjee, and K. Galsgaard (2007a), Current sheet formation and nonideal behavior at three-dimensional magnetic null points, *Phys. Plasmas*, *14*, 052106, doi:10.1063/1.2722300.
- Pontin, D. I., A. Bhattacharjee, and K. Galsgaard (2007b), Current sheets at three-dimensional magnetic nulls: Effect of compressibility, *Phys. Plasmas*, *14*, 052109, doi:10.1063/1.2734949.
- Priest, E. R., and P. Démoulin (1995), Three-dimensional magnetic reconnection without null points: 1. Basic theory of magnetic flipping, *J. Geophys. Res.*, *100*, 23,443–23,464, doi:10.1029/95JA02740.
- Priest, E. R., and T. G. Forbes (1989), Steady magnetic reconnection in three dimensions, *Sol. Phys.*, *119*, 211–214, doi:10.1007/BF00146222.
- Priest, E. R., and T. G. Forbes (2000), *Magnetic Reconnection: MHD Theory and Applications*, Cambridge Univ. Press, Cambridge, U. K.
- Priest, E. R., and V. S. Titov (1996), Magnetic reconnection at three-dimensional null points, *Philos. Trans. R. Soc. A*, *355*, 2951–2992.
- Schindler, K., M. Hesse, and J. Birn (1988), General magnetic reconnection, parallel electric fields, and helicity, *J. Geophys. Res.*, *93*, 5547–5557, doi:10.1029/JA093iA06p05547.
- Sonnerup, B. U. Ö. (1979), Magnetic field reconnection, in *Space Plasma Physics: The Study of Solar-System Plasmas*, vol. 2, 879–972, Natl. Acad. Press, Washington, D. C.
- Titov, V. S., K. Galsgaard, and T. Neukirch (2003), Magnetic pinching of hyperbolic flux tubes. I. Basic estimations, *Astrophys. J.*, *582*, 1172–1189, doi:10.1086/344799.
- Titov, V. S., T. G. Forbes, E. R. Priest, Z. Mikić, and J. A. Linker (2009), Slip-squashing factors as a measure of three-dimensional magnetic reconnection, *Astrophys. J.*, *693*, 1029–1044, doi:10.1088/0004-637X/693/1/1029.
- Tokman, M., and P. M. Bellan (2002), Three-dimensional model of the structure and evolution of coronal mass ejections, *Astrophys. J.*, *567*, 1202–1210, doi:10.1086/338699.
- Vasyliunas, V. M. (1975), Theoretical models of magnetic field line merging, *Rev. Geophys.*, *13*, 303–336.
- Wilmot-Smith, A. L., and I. De Moortel (2007), Magnetic reconnection in flux tubes undergoing spinning foot point motions, *Astron. Astrophys.*, *473*, 615–623, doi:10.1051/0004-6361:20077455.

K. Galsgaard, Niels Bohr Institute, Julie Maries vej 30, DK-2100 Copenhagen, Denmark. (kg@astro.ku.dk)
 A. L. Haynes and C. E. Parnell, School of Mathematics and Statistics, University of St. Andrews, Saint Andrews KY16 9SS, UK. (andrew@mcs.st-andrews.ac.uk; clare@mcs.st-andrews.ac.uk)